Inorg. Chem. **1992**, *31*, 4339–4345

Molybdenum(VI)–Copper(II) Schiff-Base Chain Complexes Having $Cu_2Mo_2O_4$ Cubane-like Cores. Synthesis, Crystal Structure, and Magnetic Properties of $[Cu_2Mo_2O_4(SALADHP)_2(MeO)_2{\cdot}2CH_3CN]_n$ [$H_3SALADHP$ = 1,3-Dihydroxy-2-methyl-2-(salicylideneamino)propane]

Dimitris P. Kessissoglou,[*,1a] **Catherine P. Raptopoulou,**[1a] **Evangelos G. Bakalbassis,**[1a] **Aris Terzis,**[1b] **and Jerzy Mrozinski**[1c]

Department of General and Inorganic Chemistry, Faculty of Chemistry, Aristotle University of Thessaloniki, 54006 Thessaloniki, Greece, Institute of Material Science, NRCPS Demokritos, 15310 Aghia Paraskevi Attikis, Greece, and Institute of Chemistry, University of Wroclaw, 14 F. Joliot-Curie Street, 50383 Wroclaw, Poland

Received January 24, 1992

The title compound, $Mo_2Cu_2O_4(SALADHP)_2(CH_3O)_2{\cdot}2CH_3CN$ (1), where $H_3SALADHP$ = 1,3-dihydroxy-2-methyl-2-(salicylideneamino)propane, has been prepared and its structure has been determined by X-ray crystallographic methods. Crystal data: monoclinic space group $P2_1/c$, a = 12.116 (1) Å, b = 14.112 (1) Å, c = 22.031 (2) Å, β = 116.05 (1)°, Z = 4. The structure was solved by direct methods and refined by full-matrix least-squares refinement to R = 0.0321, using 4877 reflections. The central cubane-like core of the compound can be described as a strongly distorted cube in which four corners are occupied by two copper and two molybdenum atoms. The cube is completed by four oxygen atoms from the two Schiff-base molecules and two methoxy ligands. The copper atoms are bridged by the alkoxy oxygen atoms of the SALADHP ligand with a Cu···Cu distance of 2.951 (5) Å, and the molybdenum atoms, by the methoxy oxygen atoms with a Mo···Mo distance of 3.528 (4) Å; the Mo and Cu atoms are connected by one methoxy and one alkoxy oxygen atom with an average Mo···Cu distance of 3.429 Å. The O(3) atom of the Mo═O moiety of each core has a contact to a neighboring cubane through its Cu(2) atom [Cu(2)–O(3) = 2.640 (2) Å], affording an infinite-chain arrangement. The coordination polyhedron of the Mo atom is a distorted octahedron, consisting of oxygen atoms; that of the Cu(1) atom is best described as a distorted square pyramid with a methoxy oxygen at the apex, whereas the coordination polyhedron of Cu(2) is a distorted octahedron with a significant axial elongation. The magnetic properties of the compound have been studied in the 4.2–300 K temperature range. They correspond to what is expected for a ferromagnetically coupled CuCu pair with a triplet–singlet energy gap of +30.5 cm^{-1}, being in a triply alkoxo-bridged roof-shaped Cu(II) dimer with a dihedral angle of ca. 151°. The compound shows a triplet-state room-temperature EPR spectrum.

Introduction

The complexing of two metal ions by the same macrocyclic ligand is subject to much current interest. The main reason is that such systems allow the study of metal–metal interactions; furthermore, these types of structures are found in biological systems. It is well-known that metalloproteins often use binuclear metal centers to perform catalytic functions. Moreover, both molybdenum and copper are essential elements in biological systems. The well-known antagonistic function of the molybdenum ion with regard to copper in ruminants[2] has raised interest in the interaction of Cu ions with ligated molybdenum species. However, most of the Mo–Cu mixed-metal complexes reported till now[3] employ mainly $(MoS_4)^{2-}$ as the source of the molybdenum component; moreover, these Mo–Cu mixed-metal complexes involve Mo–Cu(I) metal pairs in which the Mo most often exhibits a VI oxidation state. Mo(VI)–Cu(II) Schiff-base complexes having cubane-like cores of the formula $Mo_2Cu_2O_4$ in which Mo and Cu retain their +6 and +2 oxidation states, respectively, have not been reported in the literature. In order to expand the knowledge in this area, we have initiated a systematic synthesis and study of Mo(VI)–Cu(II) mixed-metal complexes containing pure $Mo_2Cu_2O_4$ cubane-like cores. To accomplish this, the $Mo^{VI}O_2$ Schiff-base complexes, used to study oxo-transfer reactions,[4,5] appeared to be the most appropriate Mo(VI) precursors. The present paper describes the synthesis and characterization of a series of Mo(VI)–Cu(II) mixed-metal complexes with a $Mo_2Cu_2O_4$ cubane-like core of the general formula $Mo_2Cu_2O_4$(Schiff base)$_2(CH_3O)_2$, along with the X-ray structural and magnetic analyses of the tetranuclear 2Mo(VI)–2Cu(II) system, i.e., $Mo_2Cu_2O_4(SALADHP)_2(CH_3O)_2{\cdot}2CH_3CN$, where $H_3SALADHP$ = 1,3-dihydroxy-2-methyl-2-(sali-

---

(1) (a) Aristotle University. (b) NRCPS Demokritos. (c) University of Wroclaw.

(2) (a) Mills, C. F. *Chem. Ber.* **1979**, *15*, 512. (b) Mills, C. F. *Philos. Trans. R. Soc. London, B* **1979**, *B288*, 51. (c) Bailar, J. C.; Emeleus, H. J.; Nyholm, R.; Trotman-Dickenson In *Comprehensive Inorganic Chemistry*; Pergamon: Oxford, England, 1973; Vol. 3, Chapter 36. (d) Chappell, N. R.; Kellogg. *Molybdenum in the Environment*; Marcel Dekker: New York, 1976. (e) Underwood, E. J. *Trace Elements in Human and Animal Nutrition*, 4th ed.; Academic Press: New York, 1977. (f) Clark, N. J.; Laurie, S. H. *J. Inorg. Biochem.* **1980**, *12*, 37.

(3) (a) Müller, A.; Bögge, H.; Schimanski, U. *Inorg. Chim. Acta* **1983**, *69*, 5. (b) Müller, A.; Bögge, H.; Schimanski, U. *J. Chem. Soc., Chem. Commun.* **1980**, 91. (c) Xintao, W.; Shaofeng, L.; Lianyong, Z.; Ojangjin, W. Jiaxi, L. *Inorg. Chim. Acta* **1987**, *133*, 39. (d) Shihabara, T.; Akashi, H.; Kuroya, H. *J. Am. Chem. Soc.* **1988**, *110*, 3313. (e) Müller, A.; Bögge, H.; Tölle, H.-G.; Jostes, R.; Schimanski, U.; Dartmann, M. *Angew. Chem., Int. Ed. Engl.* **1980**, *19*, 654. (f) Manoli, J. M.; Potrin, C.; Secheresse, F.; Marzak, S. *J. Chem. Soc., Chem. Commun.* **1986**, 1557. (g) Minelli, M.; Enemark, J. H.; Nicholson, J. R.; Garner, C. D. *Inorg. Chem.* **1984**, *23*, 4386.

(4) (a) Holm, R. H. *Chem. Rev.* **1987**, *87*, 1401. (b) Holm, R. H.; Berg, J. M. *Pure Appl. Chem.* **1984**, *56*, 1645. (c) Reynolds, M. S.; Berg, J. M.; Holm, R. H. *Inorg. Chem.* **1984**, *23*, 3057. (d) Berg, J. M.; Holm, R. H. *J. Am. Chem. Soc.* **1985**, *107*, 925. (e) Harlan, E. W.; Berg, J. M.; Holm, R. H. *J. Am. Chem. Soc.* **1986**, *108*, 6992. (f) Caradonna, J. P.; Harlan, E. W.; Holm, R. H. *J. Am. Chem. Soc.* **1986**, *108*, 7856. (g) Caradonna, J. P.; Reddy, P. R.; Holm, R. H. *J. Am. Chem. Soc.* **1988**, *110*, 2139. (h) Craig, J. A.; Holm, R. H. *J. Am. Chem. Soc.* **1989**, *111*, 2111. (i) Roberts, S. A.; Young, C. G.; Cleland, W. E.; Ortega, R. B.; Enermark, J. H. *Inorg. Chem.* **1988**, *27*, 3044.

(5) Craig, J. A.; Harlan, E. W.; Snyder, B. S.; Whitener, M. A.; Holm, R. H. *Inorg. Chem.* **1989**, *28*, 2082.

0020-1669/92/1331-4339$03.00/0

Chart I

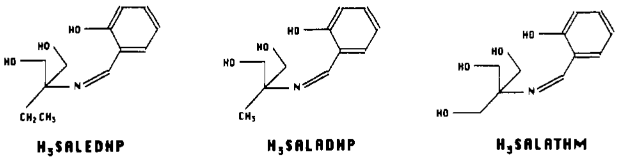

cylideneamino)propane. To our knowledge, the compound is of interest since it proves to be the first example of a Cu(II)–Mo(VI) mixed-metal linear-chain compound having pure tetranuclear $Mo_2Cu_2O_4$ cubane-like cores, the Mo:Cu ratio in the cube being 1:1 with Mo(VI) and Cu(II) oxidation states. In addition, it constitutes the first representative of a cubane-like complex containing a triply alkoxo-bridged roof-shaped Cu(II) dimer with a dihedral angle of ca. 151°; hence the interpretation of its magnetic properties is of interest too.

Experimental Section

The following abbreviations are used throughout the text (see also Chart I): $H_3SALADHP$ = 1,3-dihydroxy-2-methyl-2-(salicylideneamino)propane; $H_3SALEDHP$ = 1,3-dihydroxy-2-ethyl-2-(salicylideneamino)propane; $H_3SALATHM$ = tris(hydroxymethyl)(salicylideneamino)methane; SAL = salicylaldehyde.

Materials. Salicylaldehyde, 2-amino-2-methyl-1,3-propanediol, aminotris(hydroxymethyl)methane, and 2-amino-2-ethyl-1,3-propanediol were obtained from Aldrich, 5-chlorosalicylaldehyde (5-Cl-SAL) was obtained from Pfaltz and Bauer, and $MoO_2(acac)$, $Cu(CH_3COO)_2{\cdot}H_2O$, and $CuCl_2{\cdot}2H_2O$ were purchased from Merck. All chemicals and solvents were of reagent grade.

Physical Measurements. UV–vis spectra were recorded on a Perkin-Elmer Hitachi 200 dual-beam spectrophotometer. Infrared spectra (200–4000 cm^{-1}) were recorded on a Perkin-Elmer 467 infrared spectrometer with samples prepared as KBr pellets. Solid-state EPR spectra were recorded on a Bruker ER 200 E-SRC spectrometer. DPPH was used as an external standard. Spectra were recorded in the 0–10 000-G magnetic field range. The magnetic measurements were carried out on a polycrystalline sample of **1** by the Faraday technique in the 4.2–294 K temperature range using a sensitive RG-HV electrobalance. The applied magnetic field was 5.25 kOe, and $HgCo(SCN)_4$ was used as the susceptibility standard. The correction for the diamagnetism of the complex was estimated from Pascal constants as -390×10^{-6} cm^3 mol^{-1}; a value of 60×10^{-6} cm^3 mol^{-1} was used for the TIP of the Cu(II) ion. The magnetism of the sample was found to be field independent. Electric conductance measurements were carried out with a WTW Model LF530 conductivity outfit and a type C cell possessing a cell constant of 0.096. This represents a mean value calibrated at 25 °C with potassium chloride.

Preparation of the Complexes. Unless otherwise specified, all manipulations were performed under nitrogen with the use of standard inert-atmosphere procedures.

(a) $Cu_2Mo_2O_4(SALADHP)_2(MeO)_2$. A 20-mmol sample (2.16 mL) of salicylaldehyde was added to a solution of 20 mmol (2.10 g) of 2-amino-2-methyl-1,3-propanediol in 50 mL of MeOH. The resulting mixture was refluxed for 1 h, generating a pale yellow solution. When the solution was cooled to room temperature, 20 mmol of $MoO_2(acac)_2$ (0.625 g) was added with stirring. This pale yellow solution was refluxed for 2 h. After the reaction mixture was cooled to room temperature, it was exposed to air and allowed to evaporate slowly. A yellow crystalline solid was deposited in a few days. The crystalline product was characterized by elemental analysis and X-ray structural analysis,[6] giving the formula $MoO_2(SALADHP)(MeOH)$. A 20-mmol amount of $MoO_2(SALADHP)(MeOH)$ was dissolved in 50 mL of methanol. Onto this solution was layered 20 mL of a solution of 20 mmol of $Cu_2(CH_3COO)_4{\cdot}2H_2O$ in MeOH. After 24 h, a green crystalline product stable in the air was deposited. The crystalline product was dried under vacuum. Yield: 60%. Anal. Calcd for $Cu_2Mo_2C_{24}H_{30}N_2O_{12}$ (M_r = 857): C, 33.6; H, 3.50; N, 3.25; Cu, 14.8; Mo, 22.4. Found: C, 34.10; H, 3.65; N, 3.10; Cu, 14.10; Mo, 22.10. IR (KBr pellet, cm^{-1}): 3018 w, 2972 w, 2925 w, 2850 w, 1633 vs, 1623 vs, 1605 s, 1523 s, 1444 m, 1324 m, 1150 m, 1073 vs, 1010 s, 983 s, 943 vs, 916 vs, 889 vs, 751 m, 662 m, 555 m, 541 m, 531 m. UV–vis [λ, nm, (ε)] in CH_3CN: 650 (320), 365 (9000).

Table I. Crystallographic Data for $Cu_2Mo_2O_4(SALADHP)_2(MeO)_2{\cdot}2CH_3CN$

chem formula	$C_{28}H_{36}N_4O_{12}Cu_2Mo_2$	λ, Å	0.7107
fw	939.56	octants collcd	$+h,+k,\pm l$
space group	$P2_1/c$	μ(Mo Kα), cm^{-1}	20.23
T, °C	23	ρ_{obsd}, g cm^{-3}	1.85
a, Å	12.116 (1)	ρ_{calcd}, g cm^{-3}	1.843
b, Å	14.112 (1)	$T(max)/T(min)$	1.17
c, Å	22.031 (2)	R^a	0.0209
β, deg	116.05 (1)	$R_w{}^b$	0.0236
V, Å^3	3384.3 (2)	GOF[c]	1.53
Z	4		

[a] $R = \sum(||F_o| - |F_c||)/\sum|F_o|$. [b] $R_w = [\sum[w(|F_o| - |F_c|)^2]/\sum w|F_o|^2]]^{1/2}$. [c] GOF $= [\sum w(|F_o| - |F_c|)^2/(\text{no. of refls} - \text{no. of params})]^{1/2}$.

Crystals suitable for the X-ray structure analysis of **1** were obtained by slow evaporation of an acetonitrile solution of the green solid in about a week. Anal. Calcd for $Cu_2Mo_2C_{28}H_{36}N_4O_{12}$ (M_r = 939): C, 35.80; H, 3.85; N, 5.95; Cu, 13.50; Mo, 20.45. Found: C, 35.60; H, 3.60; N, 6.10; Cu, 13.15; Mo, 20.15.

(b) $Cu_2Mo_2O_4(5\text{-}Cl\text{-}SALADHP)_2(MeO)_2$. The procedure was identical to that described above, except that 5-chlorosalicylaldehyde was used instead of salicylaldehyde. Yield: 70%. Anal. Calcd for $Cu_2Mo_2Cu_{24}H_{28}N_2Cl_2O_{12}$ (M_r = 927): C, 31.10; H, 3.00; N, 3.00; Cu, 13.7; Mo, 21.0; Cl, 7.70. Found: C, 30.10; H, 3.15; N, 2.95; Cu, 13.20; Mo, 20.5; Cl, 7.30. IR (KBr pellet, cm^{-1}): 3020 w, 2962 w, 2920 w, 2860 w, 1620 vs, 1600 sh, 1518 s, 1450 vs, 1312 s, 1072 s, 1008 m, 980 m, 942 vs, 915 s, 888 s, 760 m, 535 m.

(c) $Cu_2Mo_2O_4(5\text{-}Cl\text{-}SALEDHP)_2(MeO)_2$. The procedure was identical to that described above, with 5-chlorosalicylaldehyde and 2-amino-2-ethyl-1,3-propanediol used as starting materials. Yield: 50%. Anal. Calcd for $Cu_2Mo_2C_{26}H_{32}N_2Cl_2O_{12}$ (M_r = 954): C, 32.70; H, 3.35; N, 2.90; Cu, 13.30; Mo, 20.10. Found: C, 33.00; H, 3.40; N, 2.80; Cu, 13.00; Mo, 20.60. IR (KBr pellet, cm^{-1}): 3045 w, 3025 w, 2975 w, 2940 w, 2880 w, 1632 vs, 1532 s, 1455 s, 1379 s, 1306 s, 1175 s, 1075 m, 1040 s, 980 w, 940 sh, 925 sh, 905 vs, 832 m, 800 s, 692 m, 650 s, 550 m.

(d) $Cu_2Mo_2O_4(SALEDHP)_2(MeO)_2$. The procedure was identical to that described above, with chlorosalicylaldehyde and 2-amino-2-ethyl-1,3-propanediol used as starting materials. Yield: 60%. Anal. Calcd for $Cu_2Mo_2C_{26}H_{34}N_2O_{12}$ (M_r = 885): C, 35.30; H, 3.80; N, 3.20; Cu, 14.40; Mo, 21.70. Found: C, 35.40; H, 3.60; N, 3.30; Cu, 14.10; Mo, 22.10. IR (KBr pellet, cm^{-1}): 3042 w, 2960 w, 2930 w, 2850 w, 1630 vs, 1620 vs, 1600 s, 1540 s, 1444 vs, 1290 s, 1200 m, 1152 s, 1040 s, 945 vs, 915 sh, 905 vs, 762 s.

(e) $Cu_2Mo_2O_4(SALATHM)_2(MeO)_2$. The procedure was identical to that described above, with 5-chlorosalicylaldehyde and tris(hydroxymethyl)aminomethane used as starting materials. Yield: 50%. Anal. Calcd for $Cu_2Mo_2C_{24}H_{30}N_2O_{14}$ (M_r = 889): C, 32.40; H, 3.40; N, 3.10; Cu, 14.30; Mo, 21.60. Found: C, 33.00; H, 3.65; N, 2.95; Cu, 14.50; Mo, 21.20. IR (KBr pellet, cm^{-1}): 3392 m, 3315 m, 3020 w, 2920 w, 2875 w, 1620 vs, 1600 s, 1540 s, 1445 s, 1300 s, 1200 m, 1155 s, 1130 m, 1085 w, 1030 vs, 982 w, 972 w, 938 m, 895 m, 860 m, 763 vs, 675 s, 662 s, 550 m, 515 m.

Crystallographic Data Collection and Structure Determination. A green parallelepipedic crystal with approximate dimensions $0.28 \times 0.31 \times 0.41$ mm was mounted in a glass capillary along with a drop of mother liquor in order to prevent the loss of solvent molecules of crystallization. Diffraction measurements were made on a $P2_1$ Nicolet diffractometer upgraded by Crystal Logic using Zr-filtered Mo radiation. The space group was determined by preliminary Weissenberg and precession photographs. Unit cell dimensions were determined and refined by using the angular settings of 26 automatically centered reflections in the range $11° < 2\theta < 24°$ and are given in Table I. Intensity data were recorded using a θ–2θ scan to $2\theta(max)$ = 50° with a scan speed of 4.5°/min and scan range of 2.0° plus the α_1–α_2 separation. Three standard reflections monitored every 97 reflections showed less than 3% variation and no decay. Lorentz, polarization, and ψ-scan absorption corrections were applied using Crystal Logic software. Scattering factors were taken from ref 7. No corrections were made for extinction.

Symmetry-equivalent data were averaged with R = 0.021 to give 5924 independent reflections from a total 6503 collected. The structure was

---

(6) Raptopoulou, C. A.; Kessissoglou, D. P.; Terzis, A. Manuscript in preparation.

(7) *International Tables for X-ray Crystallography*; Kynoch Press: Birmingham, England; Vol. IV.

Table II. Positional and Equivalent Thermal Parameters (×10⁴) for the Non-H Atoms of $Cu_2Mo_2O_4(SALADHP)_2(MeO)\cdot 2CH_3CN$

atom	*x*	*y*	*z*	U_{eq},[a] Å²
Mo(1)	6435.6 (2)	3338.4 (2)	1811.0 (1)	300
Mo(2)	4366.9 (2)	3643.1 (2)	2528.8 (1)	300
Cu(1)	4205.0 (3)	1672.7 (3)	1551.3 (2)	295
Cu(2)	6256.0 (3)	1607.8 (3)	2921.3 (2)	276
O(1)	6602 (2)	4532 (2)	1828 (1)	487
O(2)	6234 (2)	3026 (2)	1028 (1)	465
O(3)	4438 (2)	4837 (2)	2424 (1)	469
O(4)	4460 (2)	3527 (2)	3312 (1)	469
O(5)	6174 (2)	3375 (2)	2777 (1)	299
O(6)	4591 (2)	3353 (2)	1585.1 (9)	306
O(7)	6476 (2)	1499 (2)	3815 (1)	376
O(8)	6027 (2)	1795 (1)	1967.4 (9)	270
O(9)	8068 (2)	2962 (2)	2377 (1)	351
O(17)	3971 (2)	1349 (2)	683 (1)	447
O(18)	4496 (2)	2026 (1)	2489 (1)	267
O(19)	2676 (2)	3397 (2)	1983 (1)	361
N(1)	7902 (2)	1288 (2)	3089 (1)	282
N(2)	2525 (2)	1543 (2)	1393 (1)	321
C(6)	3738 (3)	3821 (3)	977 (2)	485
C(5)	7100 (3)	3748 (3)	3400 (2)	438
C(11)	7538 (3)	1358 (2)	4340 (2)	322
C(12)	7571 (3)	1295 (3)	4982 (2)	451
C(13)	8655 (4)	1162 (3)	5558 (2)	499
C(14)	9761 (4)	1092 (3)	5522 (2)	461
C(15)	9770 (3)	1147 (3)	4908 (2)	423
C(16)	8681 (3)	1262 (2)	4305 (2)	314
C(17)	8792 (3)	1228 (2)	3684 (2)	338
C(18)	8117 (3)	1224 (2)	2475 (2)	328
C(19)	6848 (3)	1132 (2)	1885 (2)	308
C(20)	8739 (3)	2132 (2)	2404 (2)	358
C(21)	8900 (3)	367 (2)	2496 (2)	426
C(31)	2890 (3)	1338 (3)	151 (2)	364
C(32)	2855 (3)	1293 (3)	−492 (2)	473
C(33)	1777 (4)	1291 (3)	−1069 (2)	508
C(34)	655 (4)	1307 (3)	−1038 (2)	509
C(35)	650 (3)	1356 (3)	−421 (2)	477
C(36)	1747 (3)	1373 (3)	184 (2)	364
C(37)	1628 (3)	1454 (3)	802 (2)	364
C(38)	2324 (3)	1676 (2)	2008 (2)	333
C(39)	3572 (3)	1512 (3)	2599 (2)	335
C(40)	1891 (3)	2688 (3)	2044 (2)	382
C(41)	1383 (3)	988 (3)	2045 (2)	448
C(2)	2844 (4)	1176 (4)	4088 (2)	678
C(1)	4168 (4)	1151 (6)	4389 (2)	1062
N(3)	1823 (4)	1202 (4)	3845 (3)	968
C(3)	8575 (4)	1262 (4)	574 (3)	802
C(4)	7569 (4)	1233 (3)	294 (2)	646
N(4)	6226 (4)	1208 (4)	−67 (2)	952

[a] $U_{eq} = (U_{11} + U_{22} + U_{33})/3$.

solved by direct methods using SHELXS-86[8a] and refined by full-matrix least-squares techniques with SHELX-76[8b] using only 4877 reflections with $F_o \geq 6\sigma(F_o)$ and refining 507 parameters. All hydrogen atoms except those of the acetonitrile molecules were located by difference maps, and their positions were refined isotropically. All non-hydrogen atoms were refined anisotropically. The methyl group hydrogens of the acetonitrile molecules were introduced at calculated positions 0.96 Å from their respective carbon atoms, and a rotation and common isotropic parameter were refined. The final values for R, R_w, and GOF for observed data are given in Table I; those for all data are 0.0321, 0.0353, and 2.07, respectively. The maximum and minimum residual peaks in the final difference map were 0.26 and −0.34 e/Å⁻³, respectively. The largest shift/esd in the final cycle was 0.26 for a hydrogen atom.

Positional and U_{eq} thermal parameters are given in Table II, and selected bond distances and angles, in Table III.

Results and Discussion

Synthesis. The synthesis of the compounds reported herein can be achieved via the pseudotemplate reaction of molybdenum(VI) acetylacetonate with SAL and 2-amino-2-methyl-1,3-propanediol, aminotris(hydroxymethyl)methane, and/or 2-amino-2-ethyl-1,3-propanediol in methanol followed by complexation with Cu(II) ions. The reactions involve deprotonation of the ligand by $MoO_2(acac)_2$ and/or $Cu(CH_3COO)_2$ in the absence of another suitable base, as follows:

$$XC_6H_3(OH)CHO + H_2NC(R)(CH_2OH)_3 + MoO_2(acac) \xrightarrow{CH_3OH} MoO_2[XC_6H_3(O)CH{=}NC(R)(CH_2O)(CH_2OH)](CH_3OH) \quad (1)$$

$$MoO_2[XC_6H_3(O)CH{=}NC(R)(CH_2O)(CH_2OH)](CH_3OH) + Cu(CH_3COO)_2 \xrightarrow{CH_3OH} Cu_2Mo_2O_4[XC_6H_3(O)CH{=}NC(R)(CH_2O)_2]_2(CH_3O)_2 \quad (2)$$

The compounds are green microcrystalline solids that appear to be air and moisture stable. They are soluble in Me_2SO, DMF, and hot CH_3CN but insoluble in methanol, CH_2Cl_2, and water. None of the complexes are electrolytes in Me_2SO, DMF, or CH_3CN.

IR Spectroscopy. The MoO_2(Schiff base)(CH_3OH) complexes exhibit two ν(O=M=O) vibrations in the 910–950-cm⁻¹ (ν_{as}) and 880–900-cm⁻¹ (ν_{sym}) regions, indicating the presence of a *cis*-MoO_2 structure. Moreover, all MoO_2(Schiff base)(CH_3OH) complexes undergo substitution reactions[6] of the type

$$MoO_2(\text{Schiff base})(CH_3OH) + L \rightarrow MoO_2(\text{Schiff base})(L) + CH_3OH$$

where L = DMSO, DMF, Py, or PPh_3. All of these complexes exhibit two *cis*-MoO_2 stretching vibrations in the 880–950-cm⁻¹ region. The corresponding $Cu_2Mo_2O_4$(Schiff base)$_2$(CH_3O)$_2$ complexes exhibit three ν(O=Mo=O) vibrations in the 940–950-, 910–920-, and 885–890-cm⁻¹ regions. The splitting of the two bands into three probably reflects the connection of one MoO_2 moiety to a Cu(II) ion of a neighboring cubane-like core in the chain.

Description of the Structure. An ORTEP diagram of **1** is displayed in Figure 1, and a packing diagram showing its 1-D infinite-chain arrangement is depicted in Figure 2. Selected bond distances and angles are given in Table III. Bond distances and angles within the SALADHP ligands are comparable to those previously found for $Mn(SALADHP)_2$[9a,b] and $Mn_3(SALADHP)_2(AcO)_4(MeOH)_2$.[9c,d]

The central cubane-like core of the compound can be described as a strongly distorted cube in which four corners are occupied by two copper and two molybdenum atoms. The cube is completed by four oxygen atoms from the two Schiff-base molecules and two methoxy ligands. The copper atoms are bridged by the alkoxy oxygen atoms of the SALADHP ligand with a Cu···Cu distance of 2.951 (4) Å, and the molybdenum atoms, by the methoxy oxygen atoms with a Mo···Mo distance of 3.528 (4) Å; the Mo and Cu atoms are connected by one methoxy and one alkoxy oxygen atom with an average Mo···Cu distance of 3.429 Å (Table III). The Cu···Cu distance is comparable to the 3.01 Å distance found within the "dimer" in the $Cu_4(EIA)_4$ [EIA = *N*-(2-hydroxyethyl)acetylacetone iminato(2−)] complex[10] with a Cu_4O_4 cubane-like core, whereas the Cu···Cu distance between the

---

[8] (a) Sheldrick, G. M. SHELXS-86: Structure Solving Program. University of Göttingen, Germany, 1986. (b) Sheldrick, G. M. SHELXS-76: Program for Crystal Structure Determination. University of Cambridge, England, 1976.

[9] (a) Kessissoglou, D. P.; Butler, W. M.; Pecoraro, V. L. *J. Chem. Soc., Chem. Commun.* **1986**, 1253. (b) Kessissoglou, D. P.; Li, X.-H.; Butler, W. M.; Pecoraro, V. L. *Inorg. Chem.* **1987**, *26*, 2487. (c) Li, X.-H.; Kessissoglou, D. P.; Kirk, M. L.; Bender, C.; Pecoraro, V. L. *Inorg. Chem.* **1988**, *27*, 1. (d) Kessissoglou, D. P.; Kirk, M. L.; Bender, C.; Lah, M. S.; Pecoraro, V. L. *J. Chem. Soc., Chem. Commun.* **1989**, 84.

[10] Bertrant, J. A.; Kelly, J. A. *Inorg. Chim. Acta* **1970**, *4*, 203.

Table III. Selected Bond Distances and Angles for $Cu_2Mo_2O_4(SALADHP)_2(MeO)_2{\cdot}2CH_3CN$

Bond Distances (Å)

Mo(1)–O(1)	1.695 (2)	Cu(1)–O(6)	2.411 (2)
Mo(1)–O(2)	1.691 (3)	Cu(1)–O(8)	1.991 (2)
Mo(1)–O(5)	2.285 (2)	Cu(1)–O(17)	1.863 (3)
Mo(1)–O(6)	2.065 (2)	Cu(1)–O(18)	2.000 (2)
Mo(1)–O(8)	2.292 (2)	Cu(1)–N(2)	1.917 (3)
Mo(1)–O(9)	1.892 (2)	Cu(2)–O(5)	2.510 (2)
Mo(2)–O(3)	1.707 (2)	Cu(2)–O(7)	1.874 (2)
Mo(2)–O(4)	1.688 (3)	Cu(2)–O(8)	2.013 (2)
Mo(2)–O(5)	2.046 (2)	Cu(2)–O(18)	2.005 (2)
Mo(2)–O(6)	2.250 (2)	Cu(2)–N(1)	1.915 (3)
Mo(2)–O(18)	2.292 (2)	Cu(2)–O(3)′	2.640 (22)
Mo(2)–O(19)	1.897 (2)	Cu(1)–O(3)′	3.350 (22)

Interatomic Distances (Å)

Cu(1)···Cu(2)	2.951 (5)	Mo(2)···Cu(2)	3.535 (5)
Mo(1)···Mo(2)	3.528 (4)	Mo(2)···Cu(1)	3.469 (5)
Mo(1)···Cu(2)	3.530 (5)	Mo(2)···Cu(2)′	4.289 (5)
Mo(1)···Cu(1)	3.435 (5)	Mo(2)···Cu(1)′	4.722 (5)

Dihedral Angles (deg)

O(8)–Cu(1)–O(18)/O(8)–Cu(2)–O(18)	29.23 (1)
Cu(1)–O_3N–mean pl/Cu(2)–O_3N–mean pl	28.88 (7)
O(8)–Cu(1)–O(18)/O(5)–Mo(1)–O(6)	13.66 (1)
O(8)–Cu(1)–O(18)/O(5)–Mo(2)–O(6)	14.61 (1)
O(8)–Cu(2)–O(18)/O(5)–Mo(1)–O(6)	17.99 (1)
O(8)–Cu(2)–O(18)/O(5)–Mo(2)–O(6)	16.78 (1)
O(5)–Mo(1)–O(6)/O(5)–Mo(2)–O(6)	11.89 (1)

Bond Angles (deg)

O(2)–Mo(1)–O(1)	104.1 (1)	O(8)–Cu(1)–O(6)	74.9 (1)
O(5)–Mo(1)–O(1)	91.2 (1)	O(17)–Cu(1)–O(6)	102.3 (1)
O(5)–Mo(1)–O(2)	159.8 (1)	O(17)–Cu(1)–O(8)	97.6 (1)
O(6)–Mo(1)–O(1)	95.8 (1)	O(18)–Cu(1)–O(6)	77.2 (1)
O(6)–Mo(1)–O(2)	95.8 (1)	O(18)–Cu(1)–O(8)	81.1 (1)
O(6)–Mo(1)–O(5)	69.3 (1)	O(18)–Cu(1)–O(17)	178.7 (1)
O(8)–Mo(1)–O(1)	166.4 (1)	N(2)–Cu(1)–O(6)	106.0 (1)
O(8)–Mo(1)–O(2)	87.8 (1)	N(2)–Cu(1)–O(8)	165.0 (1)
O(8)–Mo(1)–O(5)	75.8 (1)	N(2)–Cu(1)–O(17)	96.9 (1)
O(8)–Mo(1)–O(6)	76.3 (1)	N(2)–Cu(1)–O(18)	84.4 (1)
O(9)–Mo(1)–O(5)	85.7 (1)	O(7)–Cu(2)–O(5)	101.2 (1)
O(9)–Mo(1)–O(1)	100.6 (1)	O(8)–Cu(2)–O(7)	177.1 (1)
O(9)–Mo(1)–O(2)	103.9 (1)	O(8)–Cu(2)–O(5)	75.9 (1)
O(9)–Mo(1)–O(6)	150.3 (1)	O(18)–Cu(2)–O(5)	70.9 (1)
O(9)–Mo(1)–O(8)	82.3 (1)	O(18)–Cu(2)–O(7)	98.9 (1)
O(4)–Mo(2)–O(3)	104.5 (1)	O(18)–Cu(2)–O(8)	80.5 (1)
O(5)–Mo(2)–O(3)	96.2 (1)	N(1)–Cu(2)–O(5)	103.8 (1)
O(5)–Mo(2)–O(4)	97.3 (1)	N(1)–Cu(2)–O(7)	97.0 (1)
O(6)–Mo(2)–O(3)	91.2 (1)	N(1)–Cu(2)–O(8)	80.5 (1)
O(6)–Mo(2)–O(4)	161.2 (1)	N(1)–Cu(2)–O(18)	163.9 (1)
O(6)–Mo(2)–O(5)	70.3 (1)	Mo(2)–O(5)–Mo(1)	109.0 (1)
O(18)–Mo(2)–O(3)	165.7 (1)	Cu(2)–O(5)–Mo(1)	94.7 (1)
O(18)–Mo(2)–O(4)	88.1 (1)	Cu(2)–O(5)–Mo(2)	101.3 (1)
O(18)–Mo(2)–O(5)	75.1 (1)	Mo(2)–O(6)–Mo(1)	109.6 (1)
O(18)–Mo(2)–O(6)	75.2 (1)	Cu(1)–O(6)–Mo(1)	99.9 (1)
O(19)–Mo(2)–O(3)	101.5 (1)	Cu(1)–O(6)–Mo(2)	96.1 (1)
O(19)–Mo(2)–O(4)	101.4 (1)	Cu(1)–O(8)–Mo(1)	106.4 (1)
O(19)–Mo(2)–O(5)	150.0 (1)	Cu(2)–O(8)–Cu(1)	94.9 (1)
O(19)–Mo(2)–O(6)	85.2 (1)	Cu(2)–O(8)–Mo(1)	110.0 (1)
O(19)–Mo(2)–O(18)	82.3 (1)	Cu(1)–O(18)–Mo(2)	107.7 (1)
		Cu(2)–O(18)–Mo(2)	110.6 (1)
		Cu(2)–O(18)–Cu(1)	94.9 (1)

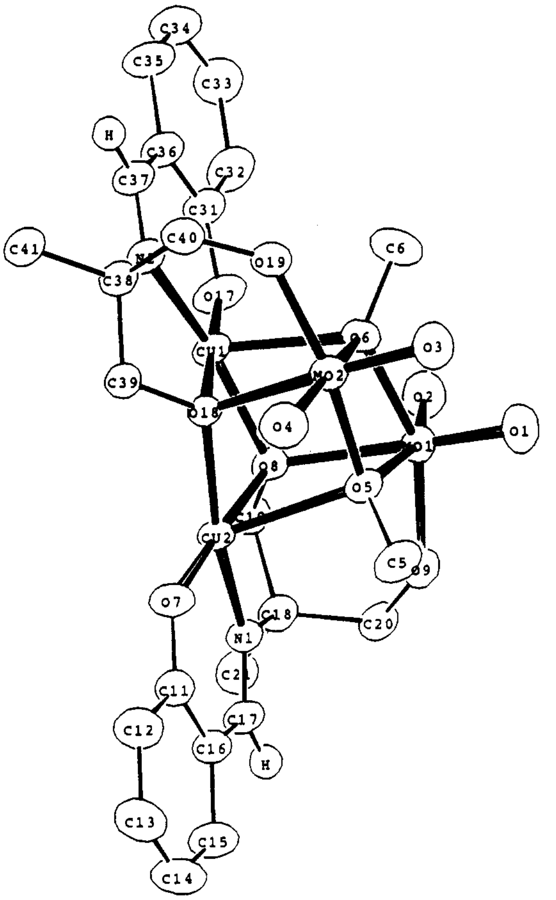

Figure 1. ORTEP diagram for **1**. Thermal motion is represented by 50% probability ellipsoids. (The CH_3CN molecules have been omitted for clarity.)

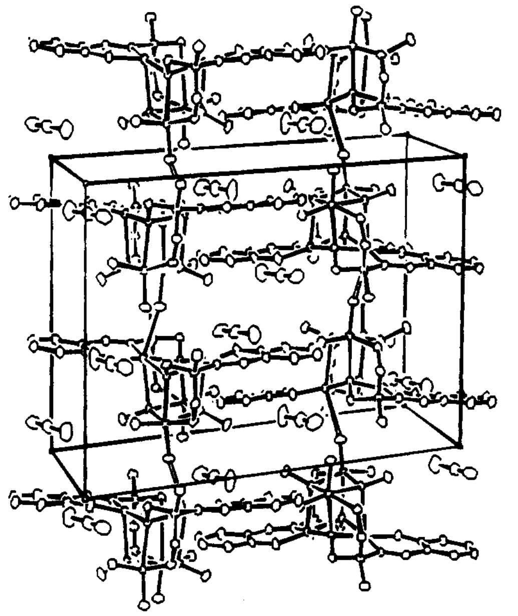

Figure 2. Packing diagram showing the 1-D infinite-chain arrangement of **1**.

"dimers" was found to be 3.26 Å, i.e. about 0.2 Å shorter than the Cu···Mo distance of 3.429 Å in our compound. The Cu···Cu distance is also in good agreement with the Ni···Ni distances within the corresponding "dimer" observed in a series of cubane-like Ni_4O_4 compounds.[11] In mixed Mo–Cu compounds with a Cu_3MoS_3Cl cubane-like core, the Cu···Cu distances are quite longer (3.10–3.29 Å) whereas the Mo···Cu distances are quite shorter (2.68–2.74 Å).[3a] The Mo···Mo distance of 3.528 (4) Å is more than 0.6 Å longer than those observed in complexes with a Mo_3CuS_4[3b–d] or Mo_4S_4[12] cubane-like core, whereas in the fused bioctahedral complex $Mo_4O_8(OC_2H_5)_2[CH_3C(CH_2O)_3]$,[13a] as well as in the series of tetranuclear Mo(VI) complexes,[13b] the

---

(11) (a) Schrauzer, G. N.; Kohnle, J. *Chem. Ber.* **1964**, *97*, 1727. (b) Adrew, J. E. *J. Chem. Soc. A* **1969**, 1457. (c) Kruger, A. G.; Winter, G. *Aust. J. Chem.* **1970**, *23*, 1. (d) Bertrand, J. A.; Ginsberg, A. P.; Kaplan, R. I.; Kirkwood, C. E.; Martin, R. L.; Sherwood, R. C. *Inorg. Chem.* **1971**, *10*, 240. (e) Vreugdenhil, W.; Haasnoot, J. G.; Reedijk, J.; Spek, A. L. *Inorg. Chim. Acta* **1987**, *129*, 205.

(12) (a) Bandy, J. A.; Davies, C. E.; Green, J. C.; Green, M. L. H.; Prout, K.; Rodgers, D. P. S. *J. Chem. Soc., Chem. Commun.* **1983**, 1395. (b) Williams, P. D.; Curtis, M. D. *Inorg. Chem.* **1986**, *25*, 4562.

Mo···Mo distances (3.30–3.60 Å) are comparable to those of the title compound. For tetranuclear complexes with a Mo_4O_4 core containing Mo(V), the Mo–Mo distances are shorter,[13c,d] only 2.600 Å, while a distance of ca. 3.24 Å spans the six face diagonals of the cube in $Mo_4O_4[(OSiCH_3)_3]_4[HN(CH_3)_2]_2$.[13e]

One of the most interesting and unusual features of this structure is the dihedral angle of 150.8° between the two O(8)–Cu–O(18) planes; this is the first example of a cubane-like complex containing a triply alkoxo-bridged roof-shaped[14] Cu(II) dimer with a dihedral angle differing so greatly from 180°. Moreover, the dihedral angle of the two O(5)–Mo–O(6) planes was found to be 168.1°. The O(3) atom of the Mo=O moiety has a contact to a neighboring cube through the Cu(2) [Cu(2)–O(3) = 2.640 (2) Å] atom, affording an infinite-chain arrangement. Distances similar to the one observed for the Cu(2)′–O(3) bond are very common for the out-of-plane oxo ligands of bis(μ-hydroxy)- and dialkoxo-bridged copper(II) compounds.[15] The two methoxy and the two alkoxy groups are triply bridging to two Cu atoms and one Mo atom and to two Mo atoms and one Cu atom, respectively. A triply bridging alkoxide group has also been observed in $Cu_4(EIA)_4$.[10]

The coordination polyhedron around each Mo atom is a distorted octahedron, consisting of oxygen atoms. The Mo–O distances are influenced by the different types of oxygen atoms. As a matter of fact, the Mo=O bond distances [1.695 (2)–1.707 (2) Å] and angles [104.1 (1) and 104.5 (1)°] of the *cis*-MoO_2 groups are within the usual ranges observed for the monomer analogs,[4,6] despite the coordination of O(3) to the Cu(2)′ of a neighboring cubane molecule. The only difference that could be assigned to this latter coordination of O(3) to Cu(2)′ is a slight elongation of the Mo(2)–O(3) bond [1.707 (2) Å] as compared to the Mo(2)–O(4) band [1.688 (3) Å] whereas the Mo(1)–O(1) and Mo(1)–O(2) bonds are almost identical [1.695 (2)–1.691 (3) Å]. The Mo–O distances of the Schiff-base alkoxy oxygens [1.892 (2) and 1.897 (2) Å] are consistent with the Mo–O distances of the monomer analog.[6] The remaining three positions of the distorted octahedron are occupied by methoxy or alkoxy triply bridging oxygens whose Mo–O distances range from 2.065 to 2.292 Å, and the angles of the trans oxygen atoms (O–Mo–O) vary from 150.0 to 166.4°. It is noticeable that the sums of the trans Mo–O distances are almost identical (3.95–3.97 Å). The lack of any elongation or depression of the octahedron also provides strong evidence that each Mo possesses a d^0 configuration with a Mo(VI) oxidation state.

The coordination polyhedron of Cu(1) is best described as a distorted square pyramid with a methoxy oxygen at the apex. The axial bond [2.411 (2) Å] is about 0.5 Å longer than the bond lengths in the basal plane [1.863 (2)–2.010 (2) Å], showing a Jahn–Teller distortion, which is consistent with a d^9 configuration of Cu and a $d_{x^2-y^2}$ ground state. Cu(1) lies almost on the basal plane [0.032-Å displacement only toward O(6)], while for the μ_4-oxo copper complexes[16] a displacement of ca. 0.23 Å has been observed. The Cu–O distance [1.863 (2) Å] of the phenoxy oxygen is about 0.13 Å shorter than those (1.99–2.00 Å) of the alkoxy bridging oxygens [O(8), O(18)] in the basal plane. The angles between the cis and trans groups in the basal plane (81.1–97.6 and 165.0–178.7°, respectively) are indicative of a square pyramidal coordination rather than a trigonal bipyramidal one.

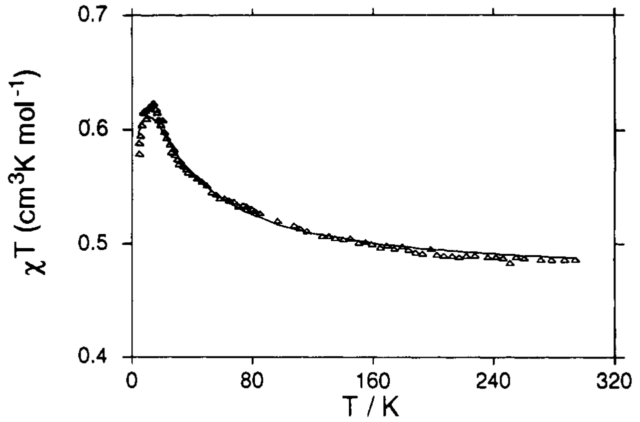

Figure 3. Experimental (triangles) and theoretical (solid line) temperature dependence (290–4.2 K) of χT (J, g, zJ' parameter fitting).

The coordination polyhedron of Cu(2) connected to a neighboring cubane through the MoO_2 moiety is best described as a distorted octahedron with a significant axial elongation. Actually, the Cu(2)–O(5) and Cu(2)–O(3)′ distances of 2.511 (2) and 2.640 (2) Å, respectively, are about 0.5–0.65 Å larger than those of the Cu(2)–O(8) [2.013 (2) Å] and Cu(2)–O(18) [2.005 (2) Å] alkoxy bridging oxygens in the equatorial plane. The observed Jahn–Teller distortion also supports a d^9 configuration for Cu(2). This atom lies almost on the equatorial plane, as its displacement is only 0.032 Å toward O(3)′ of the neighboring cubane.

Magnetic Properties. The magnetic behavior of **1**, in the form of a $\chi_M T$ vs T plot, χ_M being the magnetic susceptibility per copper(II) ion and T the temperature, is shown in Figure 3. At room temperature $\chi_M T$ is equal to 0.4866 cm³ K mol⁻¹. When the temperature is lowered from room temperature, $\chi_M T$ increases smoothly, reaching a maximum at about 14 K with $\chi_M T = 0.6227$ cm³ K mol⁻¹, and then decreases to a value of 0.5796 cm³ K mol⁻¹ at 4.2 K [full-length tables of magnetic data—experimental and calculated $\chi_M T$ values—are given as supplementary material (Table SIV)].

The interpretation of the magnetic behavior in the 4.2–290 K temperature range is straightforward. Each cubane-like core of the complex is composed of two pairs of Cu(II) and Mo(VI) ions. However, the two Mo(VI) ions are diamagnetic; hence, only the exchange parameter for the two Cu(II) interacting centers has to be considered. The exchange interaction between the two single-ion spin doublets leads to two molecular levels characterized by $S = 0$ and $S = 1$, respectively, and separated by J. J is positive if the spin triplet is the lowest level. At room temperature, the $\chi_M T$ value is already higher than that expected (ca. 0.40 cm³ K mol⁻¹) for a noncoupled copper(II) ion. The increase in $\chi_M T$ upon cooling shows that the $S = 1$ level is actually the lowest in energy. The decrease in $\chi_M T$ below ca. 14 K is most likely due to the superimposition of a very weak interdimer antiferromagnetic coupling between the $S = 1$ molecular spins on the intramolecular ferromagnetic coupling.

Considering the structure, two exchange pathways are possible: one through the O(8) and O(18) atoms bridging the two neighboring Cu(1) and Cu(2) atoms of the same cubane-like unit and the other one through the O(3) bridging two subsequent cubane-like cores. Although the crystal structure suggests a one-dimensional chain structure, the magnetic data indicate that the compound rather behaves magnetically as a chain of weakly interacting binuclear units. Therefore, a least-squares fit of the experimental data from room temperature down to 4.2 K was

---

(13) (a) Wilson, A. J.; Robinson, W. T.; Wilkins, C. J. *Acta Crystallogr., Sect. C* **1983**, *39*, 54. (b) Kang, H.; Shahid, N. S.; Nicholson, T.; Zubieta, J. *Inorg. Chem.* **1989**, *28*, 920. (c) Koch, S. A.; Lincoln, S. *Inorg. Chem.* **1982**, *21*, 2904. (d) Liu, S.; Zubieta, J. *Polyhedron* **1989**, *8*, 537. (e) Kim, G. S.; Kesler, D. A.; Dekock, C. W. *Inorg. Chem.* **1991**, *30*, 574.

(14) (a) Charlot, M. F.; Jeannin, S.; Jeannin, Y.; Kahn, O.; Lucrece-Abaul, J.; Martin-Frere, J. *Inorg. Chem.* **1979**, *18*, 1675. (b) Charlot, M. F.; Kahn, O.; Jeannin, S.; Jeannin, Y. *Inorg. Chem.* **1980**, *19*, 1411.

(15) (a) Lewis, D. L.; Hatfield, W. E.; Hodgson, D. J. *Inorg. Chem.* **1972**, *11*, 2216. (b) Lewis, D. L.; Hatfield, W. E.; Hodgson, D. J. *Inorg. Chem.* **1974**, *13*, 147. (c) McGregor, K. T.; Hodgson, D. J.; Hatfield, W. E. *Inorg. Chem.* **1976**, *15*, 421.

(16) (a) Bertrand, J. A.; Kelly, J. A. *J. Am. Chem. Soc.* **1966**, *88*, 4746. (b) Bertrand, J. A. *Inorg. Chem.* **1967**, *6*, 495. (c) Kilbourn, B. T.; Dunitz, J. D. *Inorg. Chim. Acta* **1967**, *1*, 209.

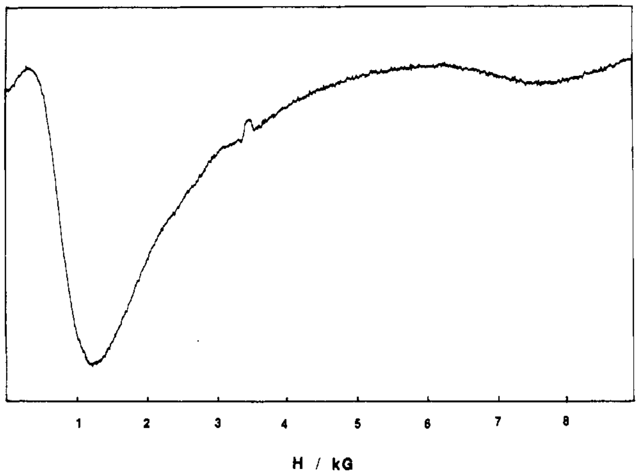

Figure 4. Room-temperature EPR powder spectrum of **1**.

attempted first in terms of a binuclear formulation via a simple Bleaney–Bowers equation.[17] The energy gap J between the triplet and the singlet state was deduced from the magnetic data through the theoretical equation

$$\chi_M = \frac{N\beta^2 g^2}{kT}[3 + \exp(-J/kT)]^{-1}$$

where N, β, k, and g have their usual meanings. J and g values were determined by minimizing the reliability factor $R = \sum_i[(\chi_{obsd})_i - (\chi_{theor})_i]^2/\sum_i(\chi_{obsd})_i^2]$, giving $J = +38$ cm^{-1} and $g = 2.215$. R was then equal to 1.74×10^{-4}, showing that a good fit was obtained when only interaction within the Cu(II) dimers inside each cubane-like core was considered. The absence of a line at ca. 3000 G in the EPR spectrum of **1** (vide infra) is in line with the absence of Cu(II) monomeric impurities, confirming further our choice concerning the dimer law used in the fitting procedure. In a second approach, the possible interaction between the Cu(II) dimers inside each cubane-like core was considered by using the molecular field approximation[18] model. In the frame of this approximation, values of +30.5 cm^{-1}, 2.241, and −0.2342 cm^{-1} were obtained for J, g, and zJ', respectively, with a better R value ($R = 8.44 \times 10^{-5}$) than that in the previous calculation (Figure 3). In the three-parameter fitting with J, g, and zJ' variables, the quality of the fit was improved, confirming both the ferromagnetic nature of the intrabinuclear interaction and the antiferromagnetic one of the interdimer interaction. Consequently, it seems quite appropriate to employ in our case the molecular field approximation, with a J' value of −0.167 cm^{-1} (for $z = 2$) proposed for **1**.

The room-temperature X-band powder EPR spectrum of **1** shown in Figure 4 is also in line with the above results. Actually, the spectrum presents two features at ca. 800 and 7500 G, which is in accordance with a dimer with an $S = 1$ ground state, in good agreement with the magnetic susceptibility results for **1**. Moreover, the existence of only two lines in the powder spectrum is indicative of $D > h\nu$ and of a strongly unaxial **D** tensor. As a matter of fact, D and E values of 0.45 ± 0.05 cm^{-1} and 0.15 ± 0.05 cm^{-1}, respectively, could be estimated[19] by assuming a g value of 2.08. The observed lines are due to the $1 \leftrightarrow 0$ transitions in the perpendicular orientations: from the y axis (800 G) and from the x axis (7500 G).

Quantum-Chemical Interpretation of the Exchange Coupling. As was shown previously, very good agreement between the observed and calculated susceptibilities down to 4.2 K is obtained by considering that **1** is formed by separate binuclear units with a small interaction between them. The origin of this behavior can be understood as follows: The coordination of Cu(1) is 4+1, with an apical Cu(1)–O(6) bond length of 2.411 (2) Å, whereas that of Cu(2) is a distorted 4+2 one, with axial Cu(2)–O(5) and Cu(2)–O(3)′ bond lengths of 2.510 (2) and 2.640 (2) Å, respectively. Hence, the unpaired electron around each copper is described by a magnetic orbital built from the $d_{x^2-y^2}$ metallic orbital pointing toward its four nearest neighbors, i.e. in both cases toward the three O atoms and the one N atom of the basal plane; hence, the spin densities on the fifth and/or the sixth axial ligand should be very weak. Consequently, the weak Cu···O axial interactions of both Cu(1) and Cu(2) should play a minor role in the exchange phenomena of the complex.

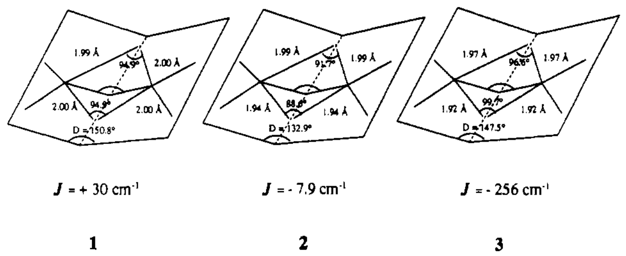

Figure 5. Structural and magnetic data of **1–3**.

The ferromagnetism of **1** is examined next. Each Cu(II) dimeric unit within each cubane-like core of **1** has a structure closely resembling that of the two roof-shaped hydroxo-bridged copper(II) binuclear complexes already reported:[14,20] $[Cu(CH_3NH_2)_2OH]_2SO_4{\cdot}H_2O$ (**2**) and $[Cu(C_6H_{11}NH_2)_2OH]_2^+$ (**3**). Moreover, the dihedral angle of ca. 150.8° for the OCuO/OCuO units of **1** is almost identical to that (ca. 151.1°) between its two basal Cu(1)–NO_3 and Cu(2)–NO_3 mean planes. The magnetic and structural results for the three complexes are shown in Figure 5. From an examination of Figure 5, the following conclusions can be drawn: Contrary to **2** and **3**, complex **1** proves to be a completely symmetric roof-shaped complex, as it possesses four equal Cu–O bonds of 2.00 Å as well as two equal Cu–O–Cu angles of ca. 94.9°; **1** is a roof-shaped alkoxo complex possessing triply bridging oxygens. In particular, each one of the bridging O(8) and O(18) atoms of each roof-shaped unit is simultaneously coordinated to three different atoms, i.e. to the two Cu(II) atoms and to a Mo(VI) atom. Moreover, the experimental J values of the actual bending structures of the same complexes are +30, −7.9, and −256 cm^{-1} for **1–3**, respectively. The question now at hand is, what is the origin of the ferromagnetism of **1** and/or why, despite their structural resemblance, does complex **3** exhibit a moderately strong antiferromagnetism of −256 cm^{-1} whereas **1** is a ferromagnetic complex?

It is well-known that antiferromagnetic interaction decreases as electron density is removed from bridging atoms.[21] Consequently, by comparing the structural features of the two complexes, one sees that the antiferromagnetism in **1** should be weaker for the following reasons: (i) The electron density on its two oxygen bridges should be reduced as compared to that in **3**, due to their triply bridging function; moreover, the longer Cu–O bonds in the Cu_2O_2 units of **1**, as compared to those in **3**, should lead to a decrease in the Cu–O overlap integrals, resulting in a further decrease in its antiferromagnetic coupling. (ii) Due to the four equal Cu–O bonds of 2.00 Å and to the two equal Cu–O–Cu angles, there is no antisynergic effect[22] that could further stabilize its singlet state as in **3**.

It should be stressed here that an analogous attenuation in the antiferromagnetic coupling, like the one reported[14,20] for **2** and **3**, has also been found for **1** upon bending of its OCuO/OCuO dihedral angle. As a matter of fact, as was shown by Kahn et al.,[14] a lowering of the J_{AF} antiferromagnetic components should

---

(17) Bleaney, B.; Bowers, K. D. *Proc. R. Soc. London, A* **1952**, *250*, 451.

(18) Ginsberg, A. P.; Lines, M. E. *Inorg. Chem.* **1972**, *11*, 2289.

(19) Gade, S.; Strand, D.; Knispel, R. *J. Magn. Reson.* **1985**, *64*, 395.

(20) Iitaka, Y.; Shimizu, K.; Kwan, T. *Acta Crystallogr.* **1966**, *20*, 803.

(21) Hay, P. J.; Thibeault, J. C.; Hoffmann, R. *J. Am. Chem. Soc.* **1975**, *97*, 4884.

(22) Mallah, T.; Boillot, M.-L.; Kahn, O.; Gouteron, J.; Jeannin, S.; Jeannin, Y. *Inorg. Chem.* **1986**, *25*, 3058.

be expected for **2** and **3** as their calculated Δ values—given in eqs 3 and 4 derived[22–24] for symmetrical binuclear complexes

$$J_{AF} = -2\Delta S \approx -S^2 \tag{3}$$

$$J_F = 2\langle \phi_A(1)\,\phi_B(2)|r_{12}^{-1}|\phi_A(2)\,\phi_B(1)\rangle = 2C \tag{4}$$

where ϕ_A and ϕ_B are the magnetic orbitals centered on A and B, respectively, S is the overlap integral $\langle\phi_A|\phi_B\rangle$, and Δ is the energy gap between the two molecular orbitals constructed from ϕ_A and ϕ_B—are lowered upon bending of the OCuO/OCuO dihedral angle. On the basis of the results of EHMO calculations performed on a model complex for **1** with the parametrization already used,[14a,21] a crossover (see also Figure 7 of ref 14a) was found for a dihedral angle of 127°. [For comparison with the analogous diagram (Figure 7 of ref 14a) valid for **2** and **3**, the model planar C_{2h} complex $[(NH_3)_2CuO\mathit{H}CH_2CH_3]_2^{2+}$ for **1** was been constructed as follows: The four actual terminal ligands were replaced by four ammonia molecules and the two bridging ligands by $^-\mathit{H}OCH_2CH_3$ groups in which *H* denotes a neutral H atom at a distance of 2.29 Å from the alkoxide oxygen atom, simulating a neutral MoL_5 metal fragment connected to the alkoxide oxygen atom in **1**].

Finally, the O(3)–Mo(2)–O(18)′ atom arrangement (see Figure 6) could easily provide the proper pathway for the propagation of the observed weak antiferromagnetism between the cubane-like cores of **1**. Due to the very weak spin density (vide supra) on O(3), this antiferromagnetic interaction should be weak.

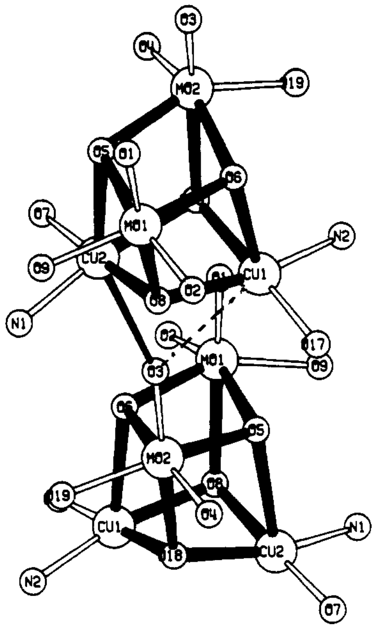

Figure 6. ORTEP diagram showing two successive cubane-like cores in the chain.

Acknowledgment. This work was supported by the Greek Ministry of Industry, Energy and Technology, General Secretariat of Research and Technology; the variable-temperature magnetic measurements were supported by KBN Project No. 2 0755 91 01. We wish to thank Dr. S. K. Hoffmann from IFN PAN, Poznan, Poland, for helpful discussions and the Department of Chemistry, University of Michigan, for use of the EPR facilities.

Supplementary Material Available: Tables SI–SIV, listing anisotropic thermal parameters of non-hydrogen atoms, positional and isotropic thermal parameters of hydrogen atoms, bond lengths and angles, and experimental and calculated magnetic susceptibility data (8 pages). Ordering information is given on any current masthead page.

Registry No. 1, 143331-89-9; 1·2CH_3CN, 143331-90-2; SAL, 90-02-8; 5-Cl-SAL, 635-93-8; 5-Cl-H_3SALADHP, 143331-86-6; 5-Cl-H_3SALEDHP, 143331-87-7; H_3SALEDHP, 143331-88-8; H_3SALATHM, 18212-81-2; $H_2NC(CH_3)(CH_2OH)_2$, 115-69-5; $MoO_2(acac)_2$, 17524-05-9; MoO_2(SALADHP)(MeOH), 143331-95-7; $Cu_2(CH_3COO)_4$, 23686-23-9; $H_2NC(CH_2CH_3)(CH_2OH)_2$, 115-70-8; $H_2NC(CH_2OH)_3$, 77-86-1; $Cu_2Mo_2O_4$(5-Cl-SALADHP)$_2$(MeO)$_2$, 143331-91-3; $Cu_2Mo_2O_4$(5-Cl-SALEDHP)$_2$(MeO)$_2$, 143331-92-4; $Cu_2Mo_2O_4$(SALEDHP)$_2$(MeO)$_2$, 143331-93-5; $Cu_2Mo_2O_4$(SALATHM)$_2$(MeO)$_2$, 143331-94-6.

---

(23) (a) Kahn, O.; Briat, B. *J. Chem. Soc., Faraday Trans. 2* **1976**, *7*, 268. (b) *Ibid.* **1976**, *7*, 1441. (c) Kahn, O.; Briat, B.; Galy, J. *J. Chem. Soc., Dalton Trans.* **1977**, 1453. (d) Girerd, J. J.; Charlot, M. F.; Kahn, O. *Mol. Phys.* **1977**, *34*, 1063.

(24) Kahn, O.; Charlot, M. F. *Nouv. J. Chim.* **1980**, *4*, 567.